

THE VIBROSEIS®* SYSTEM OF SEISMIC MAPPING

by

ROBERT L. GEYER**

INTRODUCTION

It is most important to recognize that VIBROSEIS exploration utilizes an engineered system that is based on a specific choice of input signal frequencies. Concurrent with the choice of input — *Pilot Signal* — frequencies is the obligation to support that choice of pilot signal by an equally careful choice of the other system parameters such as the source and receiver pattern geometry, group interval, and total spread length. The purpose of this essay is to review the basic principles and demonstrate some of the relations between the operating parameters.

There have been many changes in field equipment and processing systems since the first public disclosure of the VIBROSEIS system in Ponca City, April 10, 1958, and the paper by Crawford, Doty, and Lee in the February, 1960, issue of *GEOPHYSICS*. However, the principles are the same in spite of the changes from rotating weight to large truck-mounted hydraulic vibrators and from analog magnetic recording to digital field recording and data processing. The main results of such improvements are improved signal quality and much more reliable and effective field operations. To our knowledge, there has been no published tutorial description or analysis of the VIBROSEIS system as presently used after more than 10 years of field experience and development. We hope that this paper will fill that void.

BASIC PRINCIPLES

The VIBROSEIS input pilot signal is typically a swept-frequency sinusoid that lasts about six or seven seconds. The signal energy is partly reflected and partly transmitted at each elastic boundary within the earth. The transit time from the signal generator to the reflecting boundaries and back to the signal detector is generally much less than the length of the input signal. The long reflected signals overlap in time so that realistic examples tend to obscure rather than demonstrate clearly the basic principles. Therefore, we have chosen for our example not only a very simple earth model but also a very short pilot signal.

The earth model and input signal are shown in Figure 1. The earth model has three elastic boundaries or reflecting interfaces. They are labeled R_1 , R_2 , and R_3 . The reflection amplitude, which depends on the elastic contrast across the interface, can be represented graphically by a line. If we place the lines that represent the amplitudes of reflections R_1 , R_2 , and R_3 above or below a horizontal line (to represent posi-

®*Registered trademark and service mark of Continental Oil Company.

**Seismograph Service Corp., 1969.

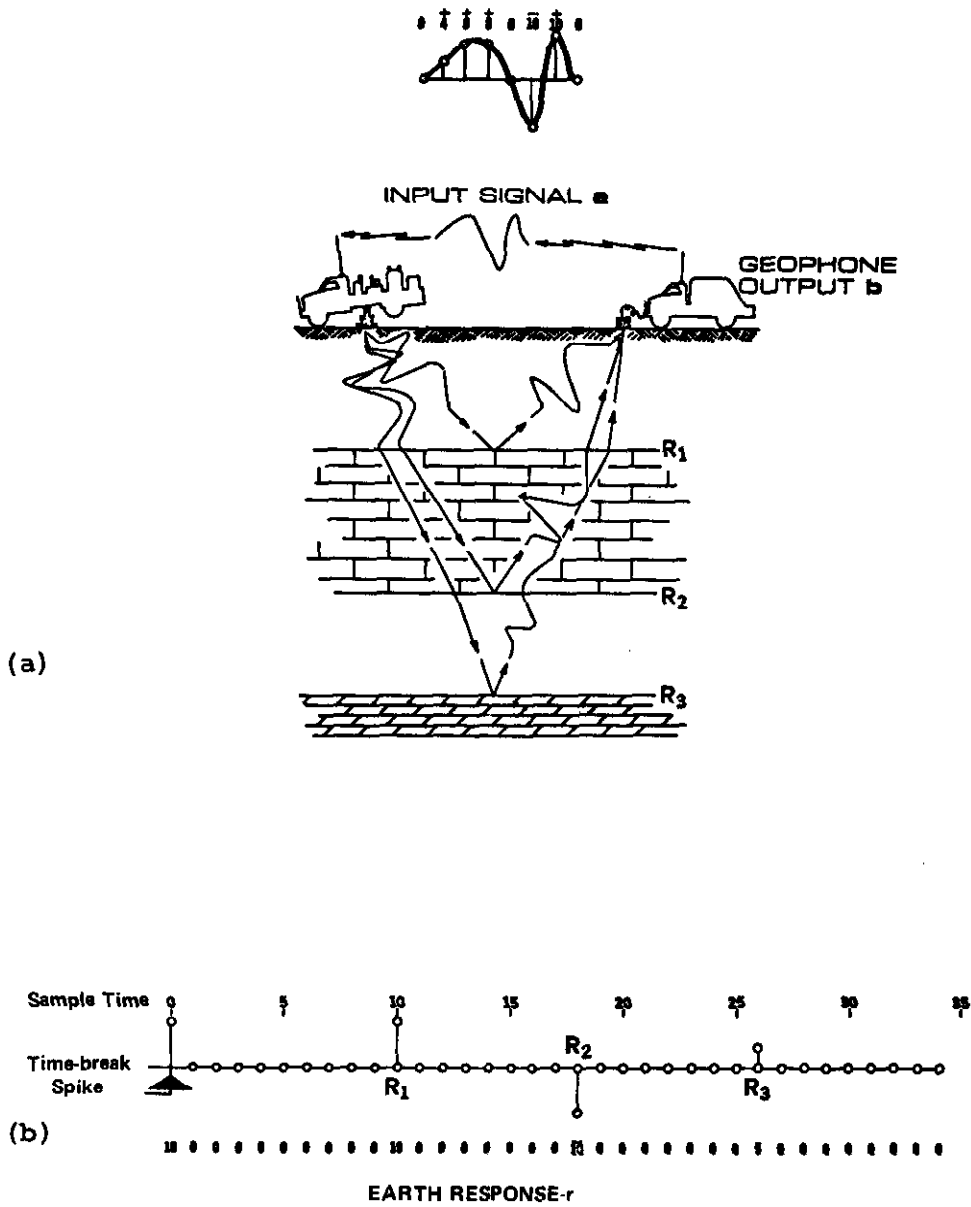


FIG. 1.—(a) Sketch of earth model with three primary reflections of input wavelet a ; (b) Earth response function r , i.e. spike synthetic seismic trace.

tive and negative polarity, respectively) and space them in proportion to their transit time we will have a time-amplitude graph. To this graph we add a line to mark the time the signal was initiated and a series of little circles to represent equal intervals of transit time. The resulting graph is a digitized, spike, synthetic seismic trace that shows the earth response to primary reflections only. This earth response trace is shown in Figure 1b.

With the earth response established, we can construct the reflection signal that the geophone sees by replacing each of the spikes on the spike trace with a replica of the input signal that has the same amplitude and polarity as the spike. The mathematical name of the replacement or substitution process is CONVOLUTION. The result for our model is shown in Figure 2c. Each replica of the input signal can be clearly distinguished because the spacing of the spikes was made greater than the length of the signal. The line was broken between the zero-time reference and geophone output to emphasize the fact that in practice they are recorded as separate signals.

As mentioned above, the usual VIBROSEIS signal is many times longer than the interval between reflections. Thus, individual reflections cannot be distinguished in the geophone output and another process is required to compress the signal to a relatively narrow wavelet or pulse. There are a number of different ways to go about compressing the pulse. The procedure used to compress the VIBROSEIS signal is called crosscorrelation. Conceptually, the geophone output is searched for replicas of the input signal, which may or may not have the same polarity, and, in general, will not have the same amplitude. The searching is done mathematically by computing a number that represents the degree of similarity between the input signal and the geophone output as one is displaced with respect to the other. When the relative position of the input signal and geophone output are shifted successively by one sample interval and the similarity factor, i.e. the correlation coefficient, is computed for each position and the resulting series of numbers is plotted graphically the result is a correlogram. If a signal is crosscorrelated with itself the result is the autocorrelation of the signal.

The result of crosscorrelating the input signal a , with the geophone output b , is shown in Figure 2e. The autocorrelation of input signal a is shown in Figure 2f. Note that the effect of the crosscorrelation has been to replace each replica of input signal a with an autocorrelation of a that has the same amplitude and polarity as the original spike of the earth response r , Figure 2a.

The basic VIBROSEIS principles can be summarized as follows.

A specified short symmetrical wavelet is substituted for the earth response by means of a two-step process: (1) a unique signal, which is longer than the transit time of the deepest reflection, is transmitted into the earth where it is convolved with the earth response to form a geophone output and (2) the long reflected signals are compressed by

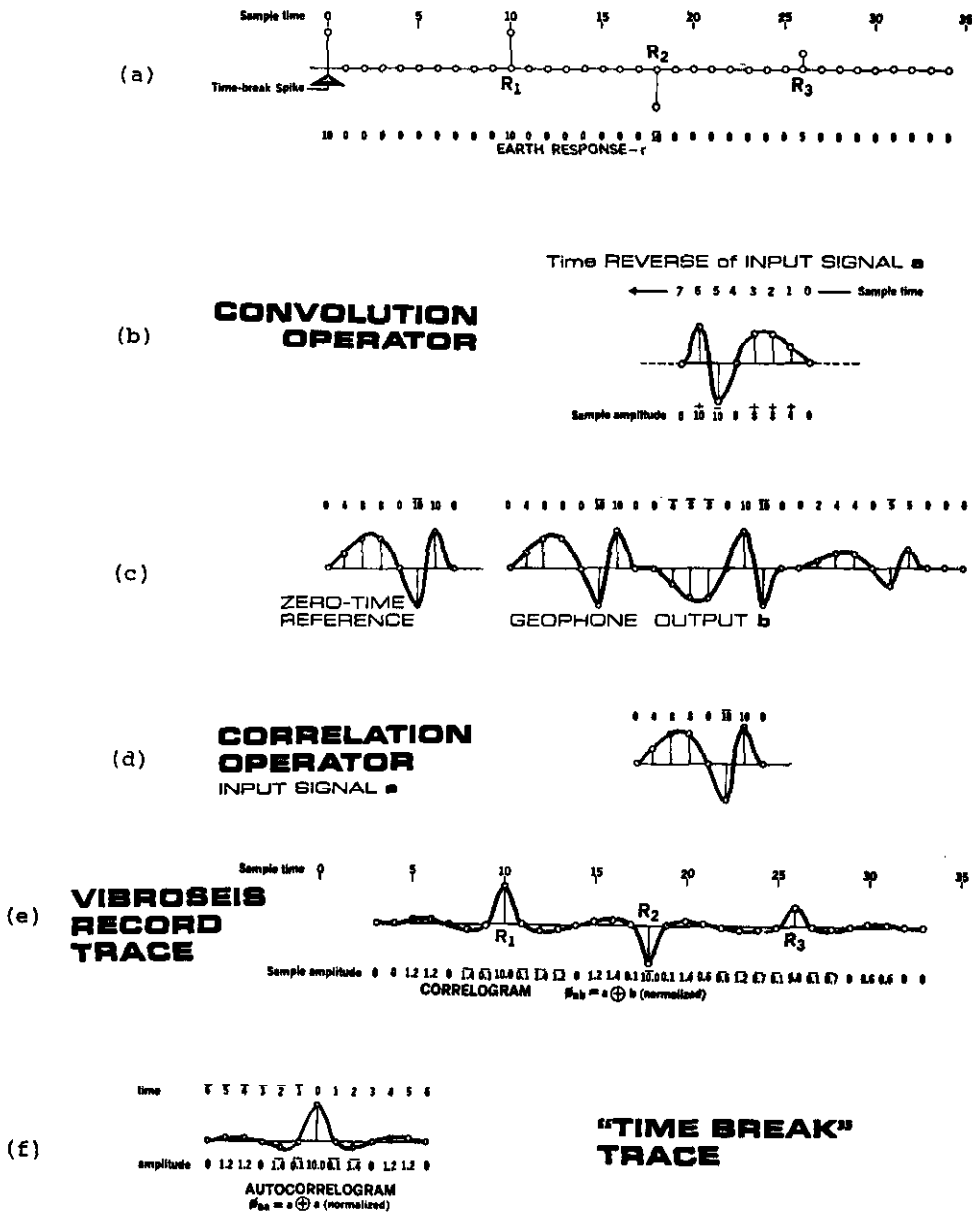


FIG. 2.—Convolution and Correlation Functions. (c) a convolved with r ; (e) crosscorrelated with b .

crosscorrelation into short symmetrical wavelets that are comparable to the wavelets from an impulsive seismic source. The characteristics of the specified short wavelet are determined by the nature of the input signal.

The principles of the VIBROSEIS system and the digital operations of convolution and crosscorrelation are demonstrated by a "slide rule" from which Figures 1 and 2 are taken.

CONVOLUTION AND CORRELATION

The slide rule to demonstrate convolution and correlation is based on the theory of convolution as described by Robinson* and an equivalent theory for correlation.

The VIBROSEIS input signal and resulting geophone output are continuous (analog) functions within certain time limits. As soon as the analog signals are sampled and converted to a sequence of numbers they become digitized discrete time functions. When two such signals are convolved or crosscorrelated, the arithmetic is simply the sums of the diagonal terms of a binary cross-product table (matrix) taken in increasing time sequence with respect to one of the signals (ordinarily the longest).

For example, let the discrete time function

$$a = (a_0, a_1, a_2), \quad (1)$$

where the subscripts denote the time sequence of the sample amplitude a , represent the input signal a . Let a second discrete time function

$$r = (r_0, r_1, r_2, r_3) \quad (2)$$

represent the earth response.

		Increasing time →			
		r_0	r_1	r_2	r_3
↓ Increasing time	a_0	$a_0 r_0$	$a_0 r_1$	$a_0 r_2$	$a_0 r_3$
	a_1	$a_1 r_0$	$a_1 r_1$	$a_1 r_2$	$a_1 r_3$
	a_2	$a_2 r_0$	$a_2 r_1$	$a_2 r_2$	$a_2 r_3$

FIG. 3.—Binary cross-product table (matrix) for time series a and r (after Robinson).

*Robinson, E. A., "Statistical Communication and Detection . . ." Charles Griffin and Company, Ltd., London, 1967.

The geophone output, which is a convolved with r , is

$$g = a * r = (g_0, g_1, g_2, \text{etc.})$$

where $*$ is the symbol for convolution of discrete time functions and the amplitudes $g_0, g_1, g_2, \text{etc.}$ are read from the binary cross-product table shown in Figure 3. The entries in the table are the products of the time-series coefficients shown in the margins. Note that the time sequence of r increases from left to right and of a from top to bottom

The convolution coefficients ($g_0, g_1, g_2, \text{etc.}$) are the sums of the cross-products in the "up-to-the-right" diagonals of the table taken in increasing time sequence with respect to time series r . Figure 4 shows how each of the convolution coefficients is related to the diagonals of Figure 3.

Note that as shown on Figure 4, when the cross-product terms are arranged in the sequence of increasing time of r the terms of a are in the sequence of decreasing time. That is, the a coefficients are in the reverse time sequence. This shows why, when we illustrate convolution graphically (as on the slide rule), the convolution operator is the time reverse of the time series that is to be substituted for each term in the series with which the operator is to be convolved.

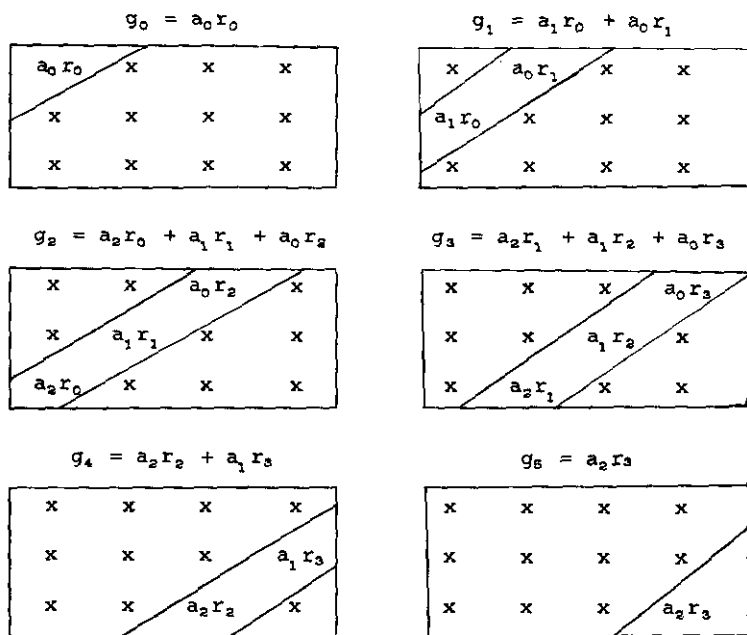


FIG. 4.—Convolution cross-product terms for successive "up-to-the-right" diagonals of the matrix shown in Figure 3. Note that the sense of the sequence of the subscript numbers of a is reversed with respect to the subscript r .

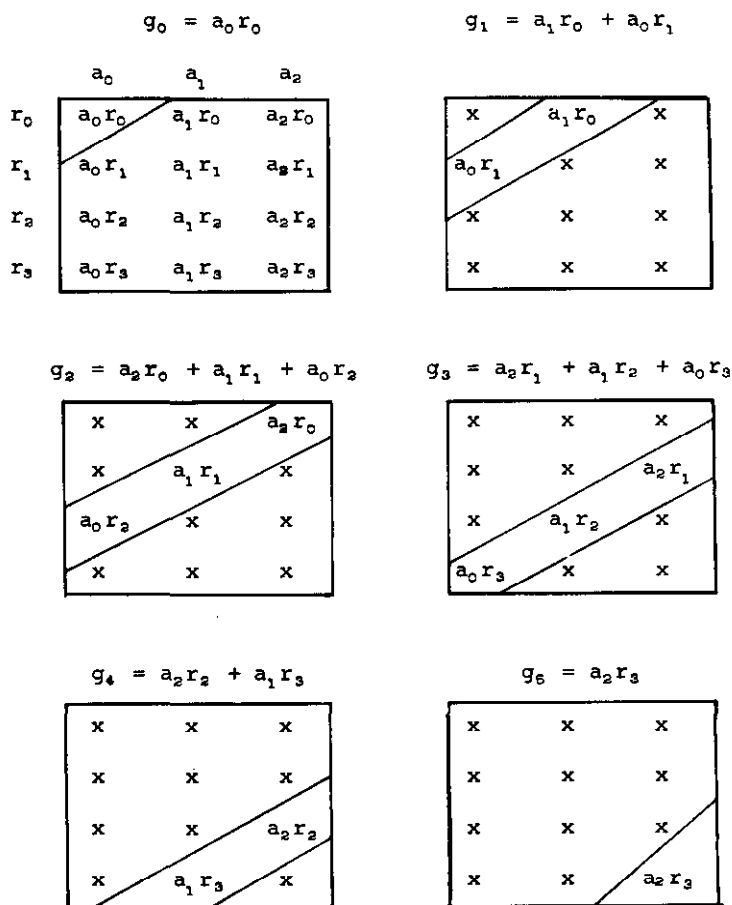


FIG. 5.—Binary cross-product matrix with locations of a and r interchanged. Note that the convolution terms are identical with those on Figure 4.

Convolution is a commutative process as shown in Figure 5 where a and r are interchanged in the binary cross-product table.

By reading the diagonals down-to-the-left in Figure 5, the sums for $g_0, g_1, g_2, g_3, g_4,$ and g_5 are easily recognized as being identical to the values shown in Figure 4. Thus, it has been demonstrated that

$$a * r = r * a. \tag{4}$$

Correlation, which is also demonstrated on the slide rule, uses the same binary cross-product table as in Figure 3 but the opposite set of diagonals as shown in Figure 6. The crosscorrelation of a and r is

$$\phi ar = a \oplus r = (\phi_0, \phi_1, \phi_2, \text{etc.}), \tag{5}$$

where \oplus is the symbol for correlation of discrete time functions. The coefficients ϕ_0, ϕ_1, ϕ_2 , etc., are the sums of the binary cross-product terms in successive down-to-the-right diagonals of the cross-product matrix. Note that, on Figure 6, when the cross-product terms are written in the sequence of increasing time of r the terms of a that occur in each product pair are likewise in the sequence of increasing time. Let us interchange the locations of a and r in the binary cross-product matrix. The result is shown in Figure 7.

The coefficients of ϕ_{ra} and ϕ'_{ar} are tabulated in Table 1 for comparison as columns 1 and 2. Examination of the values of $a \oplus r$ and $r \oplus a$ shown in columns 1 and 2, respectively, reveals the relation shown in column 3. Namely, $r \oplus a$ is the time reverse of $a \oplus r$. If

$$\phi_{ar} = a \oplus r \quad (6)$$

then

$$\phi_{ra} = r \oplus a \quad (7)$$

and

$$\phi_{ra} = \phi_{ar}(-t) \quad (8)$$

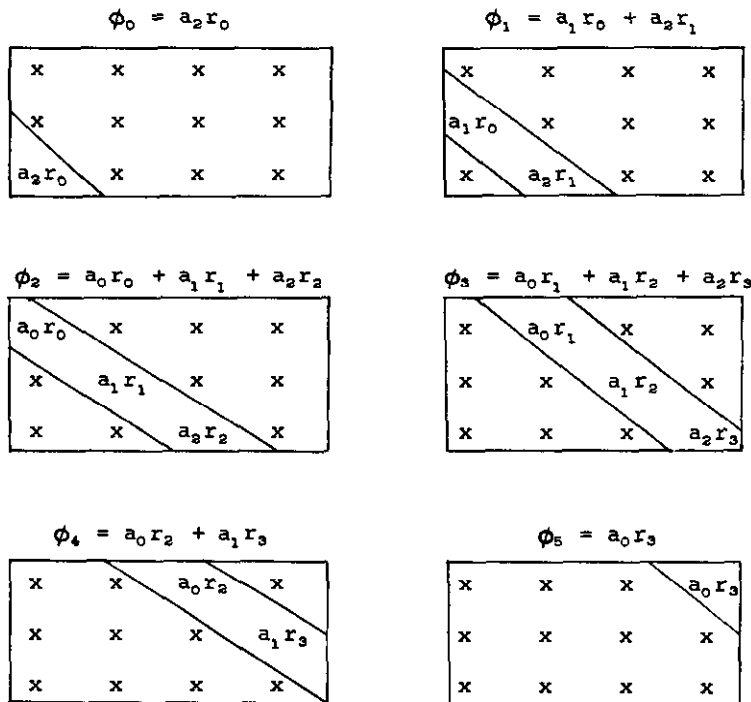


FIG. 6.—Crosscorrelation cross-product terms from successive down-to-the right diagonals of the binary cross-product matrix of Figure 3. Note that the sense of the sequence of the subscripts of a is the same as of r .

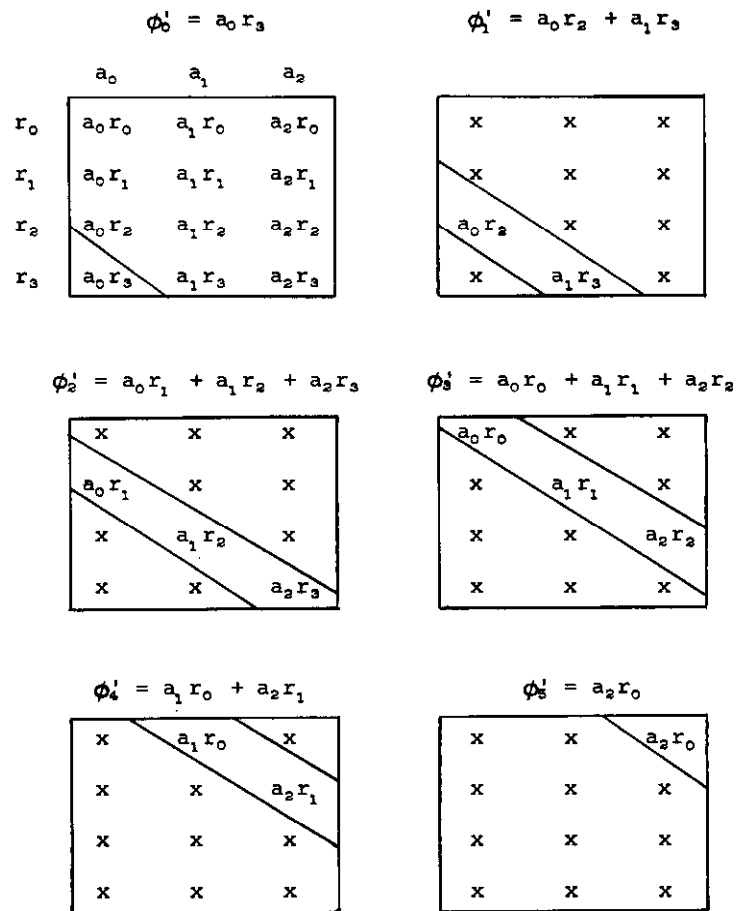


FIG. 7.—Crosscorrelation cross-product terms from matrix arrangement of Figure 5. Note that the combinations of terms in each down-to-the-right diagonal matches the terms in the diagonals of Figure 6, if the latter are taken in the reverse order.

ϕ_{ar}	$\phi'_{ar} = \phi_{ra}$	
$\phi_0 = a_2 r_0$	$\phi'_0 = a_0 r_3$	$\phi_0 = \phi'_5$
$\phi_1 = a_1 r_0 + a_2 r_1$	$\phi'_1 = a_0 r_2 + a_1 r_3$	$\phi_1 = \phi'_4$
$\phi_2 = a_0 r_0 + a_1 r_1 + a_2 r_2$	$\phi'_2 = a_0 r_1 + a_1 r_2 + a_2 r_3$	$\phi_2 = \phi'_3$
$\phi_3 = a_0 r_1 + a_1 r_2 + a_2 r_3$	$\phi'_3 = a_0 r_0 + a_1 r_1 + a_2 r_2$	$\phi_3 = \phi'_2$
$\phi_4 = a_0 r_2 + a_1 r_3$	$\phi'_4 = a_1 r_0 + a_2 r_1$	$\phi_4 = \phi'_1$
$\phi_5 = a_0 r_3$	$\phi'_5 = a_2 r_0$	$\phi_5 = \phi'_0$

TABLE 1.—Crosscorrelation cross-product terms from Figures 6 and 7 tabulated in columns 1 and 2, respectively. The equivalency is summarized in Column 3.

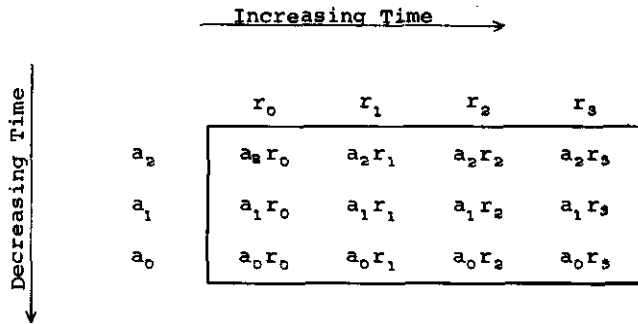


FIG. 8.—Binary cross-product matrix for $r \oplus a$. The terms in successive down-to-the-right diagonals are identical to the terms in the successive down-to-the-left convolution diagonals in Figure 4.

where the subscript (-t) denotes that the time series is reversed. Thus, the comparisons of columns 1 and 2, Table 1, show that crosscorrelation is not commutative. Note that when the terms in ϕ_{ar} and ϕ_{ra} are arranged in an increasing sequence of r the a terms are also in an increasing sequence.

Now, since convolution turns the indices of one factor around without changing the sequence of the output terms and crosscorrelation of ϕ_{ra} puts the output terms in the reverse time sequence of ϕ_{ar} , what would happen if the sequence of one set of terms was changed and then convolved with the other sequence? For example, let us reverse the order of a 's in Figure 4 and place them as shown in Figure 8. The terms of $a_{(-t)} * r$ are identical to the terms of ϕ_{ar} as listed in Table 1, columns 1 and 2. Thus, by demonstration,

$$a \oplus r = a_{(-t)} * r \quad (9)$$

and, as convolution is commutative

$$a \oplus r = r * a_{(-t)}. \quad (10)$$

INPUT-SIGNAL SPECIFICATIONS

The simple slide rule example showed that the idealized result of the VIBROSEIS system of seismic mapping is to convolve the autocorrelation function of the input signal (the autocorrelation pulse) with the earth response. That is, for each "spike" (which represents the reflection coefficient at the boundary between contiguous earth layers that have different elastic properties) in the earth response we can substitute a replica of the autocorrelation pulse with the appropriate amplitude and polarity. If we know the earth response or, in other words, if we have a "spike" synthetic trace we can get an idealized seismic trace by convolving an autocorrelation pulse with the synthetic spike trace. The characteristics of the autocorrelation pulse depend on the basic VIBROSEIS pilot-signal specifications, namely amplitude spectrum and duration of the input signal. Thus, theoretically, we can choose an input signal that will give the best resolution of the desired reflections. Inasmuch as the reflections may be the response to several adjacent interfaces the sharpest (most spikelike) autocorrelation pulse will *not necessarily* give the best seismic resolution. An input signal that has a restricted bandwidth (amplitude spectrum) can often give better resolution, i.e. reflection quality, than a broadband input signal. Therefore, an important VIBROSEIS tool is the knowledge of the fundamental relations between the input signal characteristics and the autocorrelation pulse shape. This knowledge is basic to the selection of input signals for testing or production.

Input signal characteristics

One popular VIBROSEIS input signal, which we will call an LSF input signal, is a constant amplitude (except for leading- and trailing-end taper) sinusoid that changes frequency linearly with time from some beginning frequency f_1 to some terminal frequency f_2 . The bandwidth Δ is the difference between f_1 and f_2 . If we assume that $f_2 > f_1$ then

$$\Delta = (f_2 - f_1) \text{ Hz (or cps)}. \quad (11)$$

The length of the signal in seconds is represented by T. The product $T \cdot \Delta$ is a very useful characteristic of the input signal and is called the dispersion (D). The rate of change of frequency Δ/T is represented by k. It is also convenient to define the midfrequency of the input signal as

$$f_0 = \frac{1}{2}(f_1 + f_2) \quad (12)$$

and the ratio of the terminal frequencies as

$$R_f = f_2 / f_1 \quad (13)$$

Note that the bandwidth ratio, R_f , is often expressed in "octaves" and

we speak of a one-octave or two-octave, etc., input signal. In octave notation

$$R^{\circ}_f = \frac{\log R_f}{\log 2} = \frac{\log R_f}{0.30103} \quad (\text{octaves}) \quad (14)$$

A typical linearly swept frequency signal is shown schematically by the solid wiggle line in Figure 9. The "boxcar" envelope that is assumed for discussion of signal characteristics is indicated by the rectangle. In general, the small deviation of the envelope of the actual input signal (output of the vibrator's radio receiver) from the ideal boxcar does not appreciably affect the shape of the autocorrelation wavelet as discussed below.

The analytic characteristics of the linearly swept frequency-modulated sinusoidal input signal are thoroughly examined by Klauder, et al* in a classic discussion of chirp radars.

Klauder represents the LSF or "chirp" signal by the real part of the complex waveform (Klauder Equ. (1))

$$\epsilon_1(t) = \text{rect} \left(\frac{t}{T} \right) \exp \left[2\pi i \left(f_0 t + \frac{kt^2}{2} \right) \right], \quad (15)$$

where the rectangular ("boxcar") envelope of the signal is expressed by the function $\text{rect } z$ and is defined by the relations

$$\begin{aligned} \text{rect } z &= 1, & \text{if } |z| < \frac{1}{2} \\ &0, & \text{if } |z| > \frac{1}{2} \end{aligned} \quad (16)$$

(The pulse rect has unit time duration and unit height and is centered at $t = 0$. Its spectrum is given by its Fourier transform, $\frac{\sin \pi f}{\pi f}$. The characteristics of the pulse rect are discussed by Robinson.**)

If we let S be the real part of $\epsilon_1(t)$ then

$$S = \text{rect} \left(\frac{t}{T} \right) \cos 2\pi t \left(f_0 + \frac{kt}{2} \right) \quad (17)$$

where, as previously noted, t is referred to $t = 0$ at the center of the pulse; T is the duration of the pulse; $f_0 = \frac{1}{2}(f_2 + f_1)$; and $k = \frac{\Delta}{T}$.

Although the VIBROSEIS pilot signal is generally defined by its terminal frequencies, f_1 and f_2 , and the duration, T , the expression (17)

*Klauder, J. R., Prince, A. C., Darlington, S., and Albersheim, W. J., "The Theory and Design of Chirp Radars," The Bell System Technical Journal, Vol. 39, No. 4 (July, 1960), pp. 745-808.

**Robinson, E. A., Op. Cit., pp. 58-61.

is a little easier to calculate. Therefore, f_0 and k are evaluated first and used to evaluate S .

The amplitude spectrum of the pulse (15) is obtained from its Fourier transform, which requires a tedious evaluation of complex Fresnel integrals well beyond the scope of this discussion. The interested reader will find an adequate discussion by Klauder.

Klauder wavelet characteristics

The autocorrelation of waveform (15) is given by Klauder's equ. (43) as

$$\epsilon_{mi}(t) = \frac{1}{\pi kt} e^{2\pi i f_0 t} \sin \pi (ktT - kt^2) \quad (18)$$

Equ. (18) is very useful as it can be used to easily compute the autocorrelation functions of the LSF input signal without resorting to the expensive process of crosscorrelating the signal with itself. For simplicity in discussion, the waveform represented by (18) will be called the *Klauder wavelet* (cf. Ricker wavelet). A very important application of the *Klauder wavelet* is the arbitrary waveform used to produce



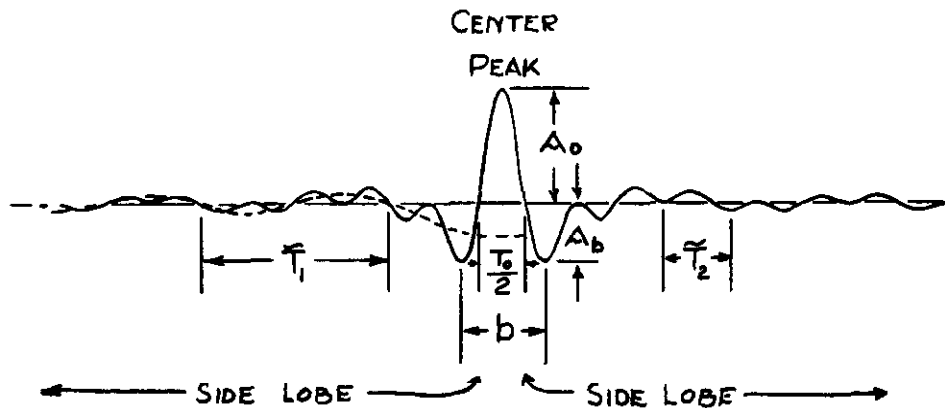
$$\text{Re } \text{rect} \left(\frac{t}{T} \right) e^{2\pi i \left(f_0 t + \frac{kt^2}{2} \right)} = S$$

$$S = \frac{t}{T} \cos 2\pi \left(f_0 t + \frac{kt^2}{2} \right)$$

$$= \cos(2\pi f_0 t) \cos(2\pi kt^2/2) - \sin(2\pi f_0 t) \sin(2\pi kt^2/2)$$

FIG. 9.—The typical VIBROSEIS LSF pilot-signal waveform and the theoretical rectangular ("boxcar") envelope.

synthetic VIBROSEIS seismic traces by convolution with the spike response obtained from an acoustic velocity log. Some of the characteristics of the Klauder wavelet are illustrated in Figure 10.



$$K = \mathcal{R}_e \left[\frac{1}{\pi kt} e^{2\pi i f_0 t} \sin \pi (ktT - kt^2) \right]$$

FIG. 10.—The "Klauder Wavelet," theoretical autocorrelation of the LSF pilot-signal obtained by evaluating Klauder's eq. (43).

The example in Figure 10 has the typical shape of the autocorrelation of a VIBROSEIS input signal that has a two-octave bandwidth. This particular Klauder wavelet was chosen for several reasons. It is one of the best for illustrating the wavelet characteristics because, in many areas, the maximum useful bandwidth of the input signal is about two octaves. And the center peak is sufficiently prominent to provide an acceptable approximation of a spike on the VIBROSEIS record (correlogram).

As can be seen, the wavelet is symmetrical about a vertical line through the center peak. If we define b_0 (the breadth of the center peak) as the absolute value of the time interval between the first + and - zero crossing points on either side of the center peak we find that

$$b_0 = \frac{T_0}{2} \quad (19)$$

where T_0 is the period of the midfrequency f_0 . Thus, we can use this same pulse shape for *any two-octave* Klauder wavelet (i.e. autocorrelation of the LSF sinusoidal input signal) by adding vertical time lines with the proper spacing. For example, if f_0 is 50 cps b_0 will be 10 millise-

onds. Therefore, the 10-ms time lines should be spaced at integral multiples of the center-peak breadth b_0 . Or, if f_0 is 25 cps b_0 will be 20 ms and the 10-ms time lines should be spaced at integral multiples of $\frac{1}{2}b_0$.

We can use the Klauder wavelet in synthesizing VIBROSEIS data as we use the Ricker wavelet in synthesizing seismic data from impulsive sources. Therefore, we define the Klauder wavelet breadth as the absolute value of the time interval between the first troughs on either side of the center peak. The pulse breadth is an easy-to-measure index of the mid- or peak-frequency of either the Ricker or Klauder wavelet. However, in neither case is it the period of the midfrequency. Although b in the Klauder wavelet is approximately twice b_0 for signals of one octave bandwidth or less, b is always less than $2b_0$ and the difference increases as the pilot-signal bandwidth increases.

The portion of the wavelet outside of the center peak is called the side lobe. The side lobe extends to the end of the wavelet and, therefore, is almost as long as the original input signal. (The autocorrelation function of a digital signal n samples long will have $2n-1$ samples. Another useful evaluation of the input signal characteristics is given by the relative amplitude of the center peak and the side lobes. If the amplitude of the center peak represents the signal on the VIBROSEIS record then the amplitude of the side lobes represents a signal-generated noise. Thus the centre peak-to-side lobe amplitude ratio represents a theoretical intrinsic signal-to-noise ratio (A_0/A_{SL}) inherent in the specifications of the input signal.

The envelope of the wavelet varies with time. The most rapid decrease in envelope amplitude occurs near the center peak because of the

factor $\frac{T}{\Delta\pi t}$. At great side-lobe times the amplitude of the envelope

decreases more slowly. The autocorrelation pulse side lobes from narrow-band (e.g. less than one-half octave) input signals have "beats" of decreasing maximum amplitude that may still be only 20 db below the center peak at a time of $20b$ after the center peak (e.g. about .700 sec after the center peak for a 1/3-octave signal and $f_0 = 30$ cps). If we define the amplitude of the first trough outside the center peak as A_b , then A_b/A_0 represents one of the most useful measures of the "spikiness" of the autocorrelation pulse. Theoretically $A_b/A_0 = 1$ where $f_2/f_1 = 1$, A_b/A_0 decreases to about one-half when f_2/f_1 is about four or one-quarter. In the case of the two-octave example $f_2/f_1 = 4$ and A_b/A_0 is about one-half.

The side lobes of the two-octave autocorrelation pulses show rather closely the normal high-frequency "ripple" in phase with the center peak and the underlying low-frequency upon which the ripple appears to be superimposed. This underlying low frequency appears to be 180° out of phase with the high frequency at the center peak time. (This apparent contradiction of the zero phase relation at zero time is related to the fact that frequencies from zero to f_1 have been omitted from the

input signal. The dashed low-frequency line does not represent the phase relation of f_1 . It is simply the "bias" upon which the high frequency f_2 appears to oscillate.) Where these two periods, T_1 and T_2 , can be recognized they give an excellent "rule-of-thumb" criteria for determining the approximate f_1 and f_2 of the input VIBROSEIS signal. The average of f_1 and f_2 , (f_0), should be very close to the value computed from the relations

$$f_0 = \frac{1}{2b_0} \text{ or } \tilde{f}_0 = \frac{1}{b} \quad (20)$$

The effect of the bandwidth of the LSF input VIBROSEIS signal on the autocorrelation pulse is shown in Figure 11. These autocorrelation

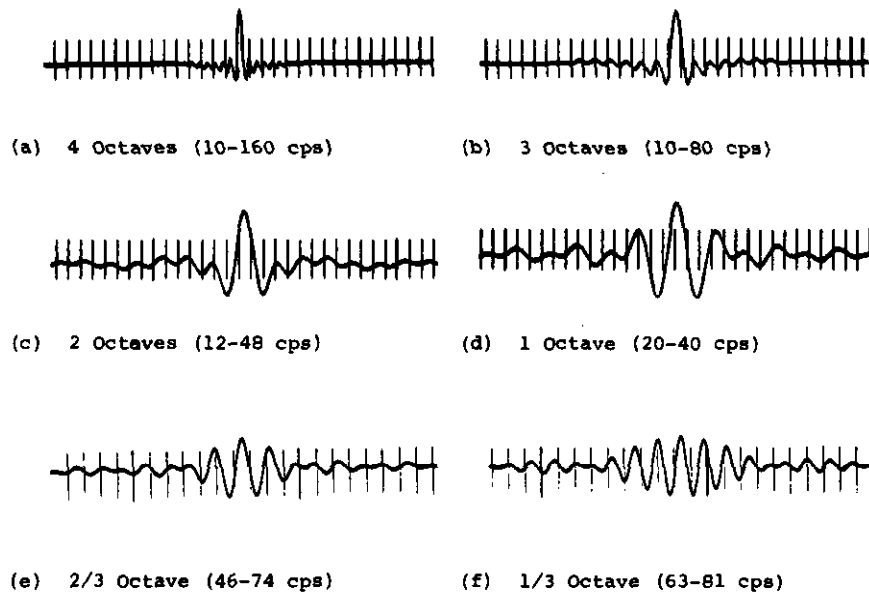


FIG. 11.—Klauder wavelets that demonstrate the effect of pilot-signal bandwidth on the autocorrelation pulse shape.

pulses are for LSF input signals of (a) four, (b) three, (c) two, (d) one, (e) two-thirds, and (f) one-third octave bandwidths. The terminal frequencies are indicated by parentheses so that the pulse shape can be related to the 10-ms time lines.

Input signals in the one- to two-octave range are among the most practicable. Broader bandwidths, which have an autocorrelation pulse that is more spike like, are more difficult to achieve in routine field practice. Input signals with narrower bandwidths have "multi-legged" autocorrelation pulses that give the VIBROSEIS record a "ringing" appearance.

It is very important to avoid mistaking the ringing caused by input signals that are too narrow with seismic ringing such as encountered frequently in marine operations. One means of distinguishing between the two kinds of ringing is a comparison of the autocorrelation of the received seismic signal. If the ringing is caused by an LSF signal that has too narrow a bandwidth the autocorrelation will resemble the pulses in Figures 11e and 11f. If the ringing is caused by seismic reverberation, the autocorrelation will have a strong side lobe at some time t_r after the center peak where t_r is the period of the reverberation. The characteristics of the autocorrelation pulses from marine reverberation are illustrated and discussed by Anstey.*

Signal-to-noise (S/N) characteristics of the LSF input signal and crosscorrelation

Up to this point, the only noise that has been discussed is the "side lobe" noise inherent in the LSF input signal bandwidth. In any seismic system there are many sources of the interference that tend to mask the "desired earth-response" signal. In this context, we define *signal* as the primary reflections from the elastic interfaces that we wish to map. *Noise*, therefore, is all of the non-signal energy that is recorded. This non-signal energy includes electrical "pickup" and instrument noise as well as all of the non-signal energy in the geophone output voltage.

The VIBROSEIS system gives us two stages for improving our S/N. The first stage is the choice of the input signal bandwidth, terminal frequencies, and duration. The second stage is the crosscorrelation process, which can further improve the S/N.

There are many kinds of seismic noise, which we may roughly classify as ambient (non-source-generated noise) and source generated noise. One of the most common and troublesome ambient noises is the 60-cps interference from electrical transmission lines (i.e. hi-line noise). Another form of ambient noise is caused by wind, especially when the seismometers are planted in grassy, brushy, or wooded areas. Airborne sound from highways, aircraft, or stationary machinery are the other main types of ambient noise.

The S/N on VIBROSEIS records (correlograms) can be improved with respect to mono-frequency signals by omitting that frequency in the input signal as, for example, by using a signal that sweeps linearly from 15 to 56 cps to reduce 60 cps hi-line interference. The crosscorrelation process provides a basic S/N improvement when the monofrequency is within the input signal bandwidth. Landrum* developed the following relations, (20) and (21), which permit a practical prediction of the S/N

*Anstey, N. A., "Correlation Display Pinpoints Seismic Multiples," Seismograph Service Limited, reprinted for circulation by Seismograph Service Corporation, 1966.

*Landrum, Ralph A., Jr., 1967, "Extraction of Signals from Random Noise by Crosscorrelation," paper at 37th Annual International Meeting of the Society of Exploration Geophysicists in Oklahoma City, Oklahoma.

improvement to be expected, and are accurate within a range of a few dB.

$$\begin{aligned} \text{S/N improvement} &= 20 [\log_{10} \sqrt{D}] \text{ dB} & (21) \\ f_1 &< f_n < f_2 \end{aligned}$$

where $D = T \cdot \Delta$, f_n = the noise frequency, and f_1 and f_2 are the terminal frequencies of the input signal. When f_n is the same as one of the terminal frequencies of the input signal the S/N improvement is twice as good, i.e.,

$$\text{S/N improvement} = 20 [\log_{10} 2 \sqrt{D}] \text{ dB} \quad (22)$$

The S/N improvement increases rapidly, generally speaking, from that given in equation (22) as the noise frequency departs farther from the signal pass band.

The crosscorrelation process is likewise a powerful tool for improving the S/N when the noise has a random pattern as produced by wind or traffic noise. The improvement resulting from crosscorrelation is

$$\text{S/N improvement} = 20 [\log_{10} \sqrt{T \cdot W}] \text{ dB} \quad (23)$$

where T is the length of the input signal in seconds, W is the bandwidth in cps of the noise (i.e. $W = f_{n2} - f_{n1}$),

$$f_{n1} < f_1, \text{ and } f_{n2} > f_1 \quad (24)$$

In general, f_{n1} will be the lower limit of the recording system, such as the seismometer cutoff frequency, for example. And, f_{n2} will be the upper limit of the recording system such as, for example, the cutoff frequency of the anti-alias filter in the amplifier. Note that, as long as W contains Δ entirely, the S/N improvement depends on the length of the input signal and is independent of the input signal frequencies or bandwidth.

Although it is not possible to express the S/N improvement quantitatively with respect to source-generated noise in general formulas, such as equations (21), (22), and (23), the same principles apply qualitatively. The most appropriate example is the improvement in S/N with respect to Rayleigh-type surface waves. In essence, such waves have very narrow frequency bandwidths. Thus, the most effective attenuation technique is to avoid the surface-wave frequencies in the input signal specification. For example, if the dominant surface-wave bandwidth is 14-18 cps choose 20 cps as the f_1 of the input signal.

In practice, of course, it is not quite that simple. In the first place the surface-wave frequencies must be determined by field tests at sites representing extremes in the velocity-layering characteristics. These tests determine the total bandwidths of the surface-wave interference to be expected over the prospect. When the surface-wave bandwidth overlaps the bandwidth of the desired signals such frequency discrimination becomes less effective as the overlap increases. However, if the field tests that give the frequencies of the surface waves are designed to give also the phase velocities, the range of wavelengths to be atten-

uated can be computed. Thus, source and receiver patterns can be designed to provide maximum attenuation for the noise wavelengths that the selected input signal will generate.

The foregoing discussion has highlighted the principles of the VIBROSEIS system of seismic exploration that lead to the selection of an input signal that will both enhance the desired reflection signals and give optimum attenuation of the undesired interference from ambient and source-generated noise. It must be emphasized that the VIBROSEIS system is not a panacea for all seismic ills. It is an engineered system that, more than any other seismic system, can be tailored to the specific signal and noise characteristics that represent the earth response of the prospect.